Composite Materials and Engineering, *Vol. 4, No. 1 (2022) 23*-41
https://doi.org/10.12989/cme.2022.4.1.023

Analytical and numerical study of failure in composite plates

Samuel N. Mula*[1], Afonso M.S. Leite[1] and Maria A.R. Loja[1,2]

[1]CIMOSM, Centro de Investigação em Modelação e Otimização de Sistemas Multifuncionais, ISEL, IPL, Instituto Superior de Engenharia de Lisboa, Av. Conselheiro Emídio Navarro 1, 1959-007 Lisboa, Portugal
[2]IDMEC, IST-Instituto Superior Técnico, Universidade de Lisboa, 1049-001 Lisboa, Portugal

(Received November 16, 2020, Revised November 22, 2021, Accepted December 7, 2021)

Abstract. In the present work, several studies related to the failure of laminated composite material plates are discussed. To carry out those studies, two models were developed: an analytical one, implemented in a symbolic computation system, MAPLE® and a numerical one implemented in ANSYS®. The main objective is the calculation of the load that originates the first ply failure in the plates studied, considering the criteria of Maximum stress and Tsai-Wu. Five case studies were considered, with different stacking sequences, different lamina thicknesses, and different arrangements and materials. Symmetrical and non-symmetrical layups were considered. The load cases comprise uniaxial and biaxial in-plane forces. The expected tension-extension and tension-bending coupling effects were also discussed.

Keywords: composite material; failure criteria; failure index; laminated plates

1. Introduction

Over the time, Mankind has developed increasingly lighter, slender, and stronger products, while having a less production time, and lower price, because of the need to achieve items with less energy consumption, better static, dynamic, magnetic, fracture, fatigue, thermal and corrosion protection properties, to cite some. Today we are offered innovative advanced design products (see e.g., Dent and Sherr 2014) at an affordable price, due to technological developments in materials, production processes and tools.

Laminated composite materials play a fundamental role in several industries, such as the aerospace, automotive, naval, biomedical, to name just a few. These materials have shown to possess several advantages such as the high strength-to-weight and stiffness-to-weight ratios, good fatigue and corrosion properties, among others, when compared to other materials. On the other hand, they present also some disadvantages, e.g., water absorption (moisture absorption) and being made of at least two materials (fibres and matrix) and produced by laying-up layer by layer, are prone to the occurrence of delamination, matrix and fibre failure, etc., when subjected to the several in-service loads.

Due to the intrinsic heterogeneous character of composite materials, failure is a complex phenomenon and often it is not possible to accurately predict the failure, as the results obtained through numerical and analytical approaches do not agree with the experimental failure mode as

*Corresponding author, Ph.D., E-mail: a42240@alunos.isel.pt

http://www.techno-press.org/?journal=cme&subpage=7 ISSN: 2671-4930 (Print), 2671-5120 (Online)

referred in Kim *et al*. (1994) and Cabrero and Gebremedhin (2010).

Liu and Tsai (1998) concluded that non-homogeneous stresses in composite structures can induce a failure scenario, in which the failure can initiate in a point of a given layer and progressively affect other layers.

Aydogdu (2008) studied the conditions for bifurcation buckling of functionally graded composite plates using the Classical Laminated Plate Theory. The authors used a clamping system to guarantee the flatness of the unsymmetrical plates under in-plane loading.

The lack of a correct understanding of the failure mechanisms, intrinsic to these complex behaviour materials, originated the creation of a worldwide exercise, named World Wide Failure Exercise-WWFE (Hinton *et al*. 2004), that is already in the third edition, focusing the laminate behaviour in 2D (WWFE I), 3D, WWFE II, referred in Kaddour and Hinton (2013) and damage and damage in the matrix, initiation of matrix-driven delamination and ultimate failure, WWFE III, referred in Kaddour *et al*. (2013).

Some criteria such as Tsai-Hill and Norris ones, assume that the tensile and compression strength are the same, which is not the case with some materials.

In the work developed by (Cabrero and Gebremedhin 2010) a literature review is performed to characterize the failure criteria and applied theories in the context of the fracture mechanics in structures made of wood. Li and Sitnikova (2018) carried out a review work which aim is to raise the awareness of rationality in the different theories so they can be appropriately applied.

Analytical models based on the Classical Laminated Plate Theory were considered in the optimization of the stacking sequence in order to maximize the strength to weight ratio (Flatscher *et al*. 2013). Camilleri *et al*. (2014) performed a comparative study considering experimental and numerical analyses for a set of composite laminates with different stacking sequences. The authors concluded that the Classical Laminated Plate Theory predicts the design load with greater precision in symmetrical and balanced plates. On the other hand, in non-symmetrical and unbalanced laminates, it was observed that the flexural stiffness promotes the strength in composite tubes.

Koc *et al*. (2016) investigated the failure behaviour of fibre-reinforced composites under four-point bending, using the Classical Laminated Plate Theory. Those authors also considered the use of the finite element method. Thermal residual stresses were calculated and accounted for in the failure analysis.

The study of the volume fraction of the fibres, fibre orientation and stacking sequence in composite materials was addressed by Nyambeni and Mabuza (2018), as design variables in a wide variety of pressure vessels, plates, and tubes, having a great influence on the response of composite structures. They also carried out a study on the influence of thermomechanical loads in the failure of those composite structures. Other works in the field of composite materials related to the present one were presented by several researchers among them, Saravanan *et al*. (2019).

The present work presents a parametric study that considers the influence of material and geometrical parameters (stacking sequences, symmetric and non-symmetric) in the failure index associated to a set of failure criteria, namely the Maximum stress and Tsai-Wu criteria.

Analytical and numerical approaches were adopted for this purpose, using respectively MAPLE® and ANSYS® APDL softwares.

2. Methodology

2.1 Constitutive equations

In order to make it possible to carry out the studies it was necessary to determine a set of

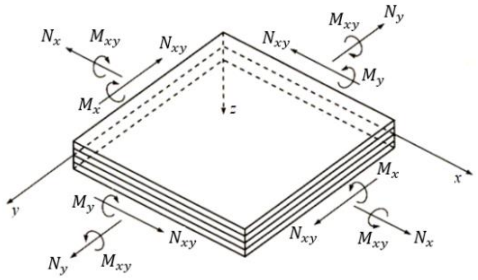

(a)

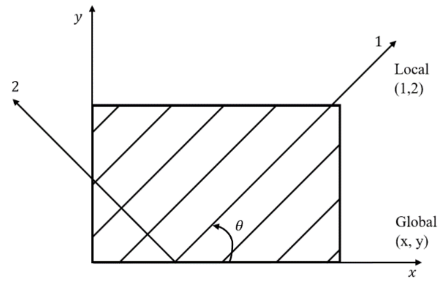

(b)

Fig. 1 Scheme of the laminate with loads and the lamina: (a) Laminate with forces and moments, (b) Unidirectional lamina and its axes: material/local (1, 2) and global (x, y)

fundamental parameters such as the states of stress and deformations acting on the laminates, among others. Through the Classical Laminated Plate Theory (CLPT) or the First-Order Shear-Deformation Theory (FSDT) for example, it is possible to relate the load applied to the plates and the stress and strain states. The loads can be applied in the plane defined by the x, y directions (see Fig. 1(b)) namely through the forces (N_x, N_y or N_{xy}) or out-of-the plane, by employing the moments M_x, M_y or M_{xy}; and also in a combined manner (see Fig. 1(a)).

According to (Reddy 1997) the resultant generalized forces per unit length $\{N\} = \{N_x, N_y \text{ or } N_{xy}\}$ and $\{M\} = \{M_x, M_y \text{ or } M_{xy}\}$ associated to the CLPT can be written as

$$\begin{bmatrix} \{N\} \\ \{M\} \end{bmatrix} = \begin{bmatrix} [A] & [B] \\ [B] & [D] \end{bmatrix} \cdot \begin{bmatrix} \{\varepsilon^0\} \\ \{k^0\} \end{bmatrix} \tag{1}$$

where $[A]$, $[B]$ and $[D]$ are respectively the membrane stiffness, the membrane-bending coupling stiffness, and the bending stiffness matrices. The associated coefficients A_{ij}, B_{ij} and D_{ij} are calculated according to

$$\left(A_{ij}, B_{ij}, D_{ij}\right) = \sum_{k=1}^{N} \int_{z_k}^{z_{k+1}} \bar{Q}_{ij}{}^{(k)} (1, z, z^2)\, dz \tag{2}$$

The coefficients $\bar{Q}_{ij}$ correspond to the transformed reduced elastic stiffness coefficients for the k^{th} layer, given in literature, namely in Reddy (1997) and (Nyambeni and Mabuza 2018). According to the CLPT displacement field, given in Eq. (3)

$$\begin{Bmatrix} u(x,y,z) \\ v(x,y,z) \\ w(x,y) \end{Bmatrix} = \begin{Bmatrix} u^0(x,y) \\ v^0(x,y) \\ w^0(x,y) \end{Bmatrix} + z \begin{Bmatrix} \theta_x^0 \\ \theta_y^0 \\ 0 \end{Bmatrix} \tag{3}$$

where the degrees of freedom u^0, v^0 and w^0 stand for the midplane displacements along the x, y and z directions and θ_x^0, θ_x^0 for the rotations around the y and x axis respectively. By considering the kinematical relations of the elasticity theory for small deformations, and the displacement field, one achieves the strain field in Eq. (4)

$$\begin{Bmatrix} \varepsilon_x \\ \varepsilon_y \\ \gamma_{xy} \end{Bmatrix} = \begin{Bmatrix} \varepsilon_x^0 \\ \varepsilon_y^0 \\ \gamma_{xy}^0 \end{Bmatrix} + z \begin{Bmatrix} k_x^0 \\ k_y^0 \\ k_{xy}^0 \end{Bmatrix}$$
$$\{\varepsilon\} = \{\varepsilon^0\} + z\{k^0\} \tag{4}$$

The strain coefficients, ε_x^0, ε_y^0 e γ_{xy}^0 represent the midplane membrane and in-plane shear deformations, and k_x, k_y and k_{xy} express the corresponding midplane curvatures. These strains can thus be related to the stresses through the constitutive relation in Eq. (5)

$$\begin{Bmatrix} \sigma_x \\ \sigma_y \\ \sigma_{xy} \end{Bmatrix} = \begin{bmatrix} \bar{Q}_{11} & \bar{Q}_{12} & \bar{Q}_{16} \\ \bar{Q}_{12} & \bar{Q}_{22} & \bar{Q}_{26} \\ \bar{Q}_{16} & \bar{Q}_{26} & \bar{Q}_{66} \end{bmatrix} \begin{Bmatrix} \varepsilon_x \\ \varepsilon_y \\ \gamma_{xy} \end{Bmatrix} \tag{5}$$

This constitutive relation, and therefore the stress state obtained, can be written in the material reference frame, and then be considered in the context of the failure criteria selected.

2.2 Composite materials' failure criteria

Typically, laminated plate failure occurs when the applied load exceeds material limits. Thus, the establishment of failure criteria plays a fundamental role, as they will allow predicting the occurrence of the first failure in these structures, regardless the complexity of the state of stress and strain the structure is undergoing.

Several failure criteria have been developed, with the objective of better characterizing and anticipating the failure occurrence in laminates. Some of these criteria neglect the interactions among different stress components and thus they are commonly described as one inequality that is established for each of the three in-plane stresses, as is the case for example of the maximum stress criterion. Other stress criteria instead, consider the interaction among different stress components.

The maximum stress criterion is also physically based, i.e., it tests each stress condition, for example the stress in the fibre direction or in the matrix direction. When it predicts failure, one knows which condition has failed. The second group of criteria is where the phenomenological criteria pertain, like Tsai-Hill and Tsai Wu. They are ruled by an equation, easy to apply, but they only detect the failure occurrence, not what was the failing mode, at least explicitly. Those criteria like Tsai-Hill can also provide erroneous results in some cases, see París (2001).

In the present work, which aims performing a comparative study for a set of typical laminated plates, one started by considering one criterion that belongs to the first group and another that pertain to the second group, respectively the maximum stress criterion and the Tsai-Wu criteria.

In general terms, the first failure prediction is based on the calculation of metrics namely the failure index and the strength ratio. According to (Barbero 2007) and (Koh and Madsen 2018), the first ply failure can be predicted by the failure index, which is given as

$$I_F = \frac{\text{Stress (generated by applied loads)}}{\text{Strength}} \tag{6}$$

The first failure is expected to occur whenever $I_F \geq 1$. The strength ratio is the inverse of the failure index, being given as

$$R = \frac{1}{I_F} = \frac{\text{Strength}}{\text{Stress (generated by applied loads)}} \tag{7}$$

According to the strength ratio, the failure is expected to occur when $R \leq 1$.

Although the selected criteria to develop the present study can predict the occurrence of the first failure, in one or several laminae, they are not able to follow the propagation of the failure until the rupture of the plates. However, they agree with the objective of the present study having in addition a low computational cost.

In the next sub-section, one summarizes the fundamentals about the Maximum Stress and the Tsai-Wu criteria, the two failure criteria that will be considered in the present work. The decision to use only those two criteria is related to the fact that (1) ANSYS® APDL has only these two criteria available, and (2), one is physically based (Maximum stress Criterion), and the other is phenomenological and polynomial (Tsai-Wu).

2.2.1 Maximum stress criterion

Considering the stress tensor defined in the material coordinates' system (Fig. 1(b)), where direction 1 coincides with the fibre direction, direction 2 is the in-plane fibre's transverse direction and the direction 3 is the ply's out-of-plane normal direction, this criterion states that the first ply failure will occur if the failure index I_F determined as given in Eq. (8) yields a value greater than 1 as mentioned (Li and Sitnikova 2018)

$$I_F = \max \begin{cases} \sigma_1/F_{1t} & if\ \sigma_1 > 0 \quad or \quad -\sigma_1/F_{1c} \quad if\ \sigma_1 < 0 \\ \sigma_2/F_{2t} & if\ \sigma_2 > 0 \quad or \quad -\sigma_2/F_{2c} \quad if\ \sigma_2 < 0 \\ \sigma_3/F_{3t} & if\ \sigma_3 > 0 \quad or \quad -\sigma_3/F_{3c} \quad if\ \sigma_2 < 0 \\ abs(\sigma_4/F_4) & \\ abs(\sigma_5/F_5) & \\ abs(\sigma_6/F_6) & \end{cases} \tag{8}$$

where $\sigma_i, i = 1..6$ denotes the normal and shear stresses and F_{ik} expresses the corresponding strength values of a unidirectional laminae. In the three first set of relations, the subscript k stands for the reference to the tension (t) or compression (c) state depending on the actual situation. This formulation is simplified to the relations involving σ_1, σ_2 and σ_6 in the case of a plane stress state in the material reference frame.

2.2.2 Tsai-Wu criterion

According to (Koh and Madsen 2018) and (Barbero 2007), the Tsai-Wu criterion (1971), Liu and Tsai (1998) emerged in order to obtain more accurate results that could better represent the experimental data, which yielded the following expression for the failure index

$$I_F = \frac{1}{\left[\frac{-B}{2A} + \sqrt{\left(\frac{B}{2A}\right)^2 + \frac{1}{A}}\right]} \tag{9}$$

where parameters $A,\ B$ are given as

$$\begin{aligned} A &= \frac{{\sigma_1}^2}{F_{1t}F_{1c}} + \frac{{\sigma_2}^2}{F_{2t}F_{2c}} + \frac{{\sigma_3}^2}{F_{3t}F_{3c}} + \frac{{\sigma_4}^2}{{F_4}^2} + \frac{{\sigma_5}^2}{{F_5}^2} + \frac{{\sigma_6}^2}{{F_6}^2} \\ &+ c4\frac{\sigma_2\sigma_3}{\sqrt{F_{2t}F_{2c}F_{3t}F_{3c}}} + c5\frac{\sigma_1\sigma_3}{\sqrt{F_{1t}F_{1c}F_{3t}F_{3c}}} + c6\frac{\sigma_1\sigma_2}{\sqrt{F_{1t}F_{1c}F_{2t}F_{2c}}} \\ B &= \sigma_1\left({F_{1t}}^{-1} - {F_{1c}}^{-1}\right) + \sigma_2\left({F_{2t}}^{-1} - {F_{2c}}^{-1}\right) + \sigma_3\left({F_{3t}}^{-1} - {F_{3c}}^{-1}\right) \end{aligned} \tag{10}$$

and $c4, c5, c6$ are the Tsai-Wu coupling coefficients. When considering a plane stress state in the ply plane, the criterion expression becomes simplified as

$$I_F = \frac{\sigma_1^2}{F_{1t}F_{1c}} + \frac{\sigma_2^2}{F_{2t}F_{2c}} + \frac{\sigma_{12}^2}{S^2} + \left(\frac{1}{F_{1t}} - \frac{1}{F_{1c}}\right)\sigma_1 + \left(\frac{1}{F_{2t}} - \frac{1}{F_{2c}}\right)\sigma_2 - \frac{\sigma_1\sigma_2}{\sqrt{F_{1t}F_{1c}F_{2t}F_{2c}}} \tag{11}$$

where the σ_i stresses and the F_{ik} strengths have the same meaning as previously mentioned.

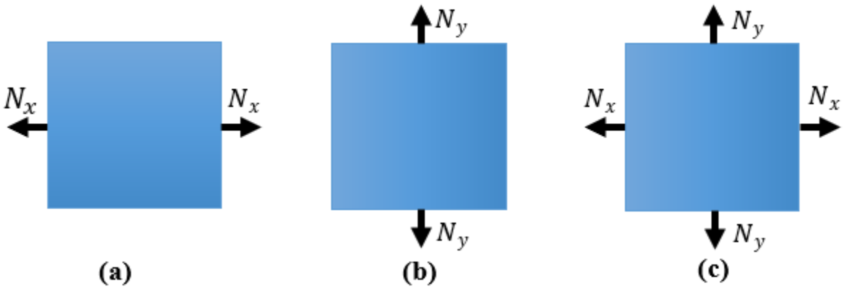

Fig. 2 Plates' loads considered. (a) Uniaxial tension along x, N_x, (b) Uniaxial tension along y, N_y and (c) Biaxial tension N_x and N_y

Table 1 Conditions related to the case studies analysed (Kaddour *et al*. 2014)

Case	Laminate distribution	Ply thickness [mm]	Material	Loading
E1	$[0^\circ_2/90^\circ_2]_S$	0.125	AS4/3501-6	
E2	$[30^\circ/90^\circ/-30^\circ/30^\circ]$	0.25		N_x
E3	$[45^\circ/-45^\circ]_S$		Glass/epoxy	N_y
E4	$[0^\circ/90^\circ/0^\circ]$	0.125		$N_x = N_y$
E5	$[0^\circ/-45^\circ/45^\circ/90^\circ]_S$	0.14	G4-800/5260	

Table 2 Materials' mechanical properties and strength parameters (Flatscher *et al*. 2013, Soden *et al*. 1998, Kaddour *et al*. 2014)

Description	Symbol	Unit	AS4/3501-6 (Graphite/Epoxy)	Glass/epoxy (Glass fibres/LY556)	G4-800/5260
Longitudinal elasticity modulus	E_1	GPa	126	45.6	173
Transverse elasticity moduli	$E_2 = E_3$		11.0	16.2	10.0
Shear moduli	$G_{12} = G_{13}$		6.6	5.83	6.94
	G_{23}		3.618	5.7	3.355
Poisson's coefficient	$v_{12} = v_{13}$	-	0.28	0.278	0.33
	v_{23}		0.396	0.40	0.49
Longitudinal tensile strength	F_{1t}	MPa	1950	1280	2750
Longitudinal compression strength	F_{1c}		1480	800	1700
Transversal tensile strength	$F_{2t} = F_{3t}$		48	40	75
Transversal compression strength	$F_{2c} = F_{3c}$		200	145	210
Shear strength	F_6		79	73	90

2.3 Implementation

The analytical model and corresponding failure criteria codes were implemented in the symbolic computation system MAPLE®, and the numerical model based on the finite element method was implemented in ANSYS® using its parametric design language (APDL).

The load conditions considered for the five case studies, addressed in the present work, are summarized in Fig. 2.

The analytical model is based on the CLPT theory and the constitutive relations of Sec. 2.1 along with the failure criteria in sec. 2.2 were implemented in MAPLE®. The failure and strength indexes were determined for a set of 1000 mm edge square plates presenting different stacking sequences. Several verification studies were first developed for cases already considered by other authors.

All the plates were discretized into 15×15 finite element meshes along the x, y directions, using the SHELL281 finite element. This finite element is based on the first-order shear-deformation theory, which considering the aspect ratio of the plates to be studied, is still within its application domain, as it is the classical theory. This discretization was selected upon a preliminary convergence study where one has concluded it already provided a good relation between the computational cost and the agreement with different reference results.

A set of five case studies were selected, based on the work developed by (Kim *et al*. 1994) and (Kaddour *et al*. 2014), to observe and characterize the laminates' behaviour under different materials, stacking sequences and boundary and loading conditions (see Table 1).

The five case studies consider different materials, whose mechanical properties and strength parameters are given in Table 2.

3. Applications

This section presents a set of case studies, which material and other characteristics were defined in the implementation subsection, in Tables 1-2. In order to simplify the simulation process, the minimum force was previously calculated for each case study so that the failure rate was approximately 0.5. The load that causes the first failure was calculated by adding 30% to the value of the last load that does not cause the plate to fail, for all the case studies (see Table 5) presented in this work. The next subsections present the results obtained concerning the evolution of the failure index with the applied load for the different loading situations.

3.1 Laminate E1 ($[0^{\circ}{}_2/90^{\circ}{}_2]_S$, AS4/3501-6)

Table 3 Comparison between analytical and numerical (Tsai-Wu criterion) approaches (Laminate E1 ($[\mathbf{0^{\circ}{}_2/90^{\circ}{}_2}]_S$, AS4/3501-6)

Analytical					Numerical				
Worst layer	3^{rd}-6^{th} (90°)	1^{st}-2^{nd} (0°)	All (0° and 90°)			3^{rd}-6^{th} (90°)	1^{st}-2^{nd} (0°)	All (90° and 0°)	
	N_x	N_y	$N_x = N_y$			N_x	N_y	$N_x = N_y$	
Load [N/mm]	I_F	I_F	Load [N/mm]	I_F	Load [N/mm]	I_F	I_F	Load [N/mm]	I_F
0	0	0	0	0	0	0	0	0	0
150.0	0.499	0.499	120.0	0.438	150.0	0.499	0.499	120.0	0.438
195.0	0.648	0.648	156.0	0.569	195.0	0.648	0.648	156.0	0.569
253.5	0.843	0.843	202.8	0.740	253.5	0.843	0.843	202.8	0.740
329.6	1.095	1.095	342.7	1.251	329.6	1.095	1.095	342.7	1.251

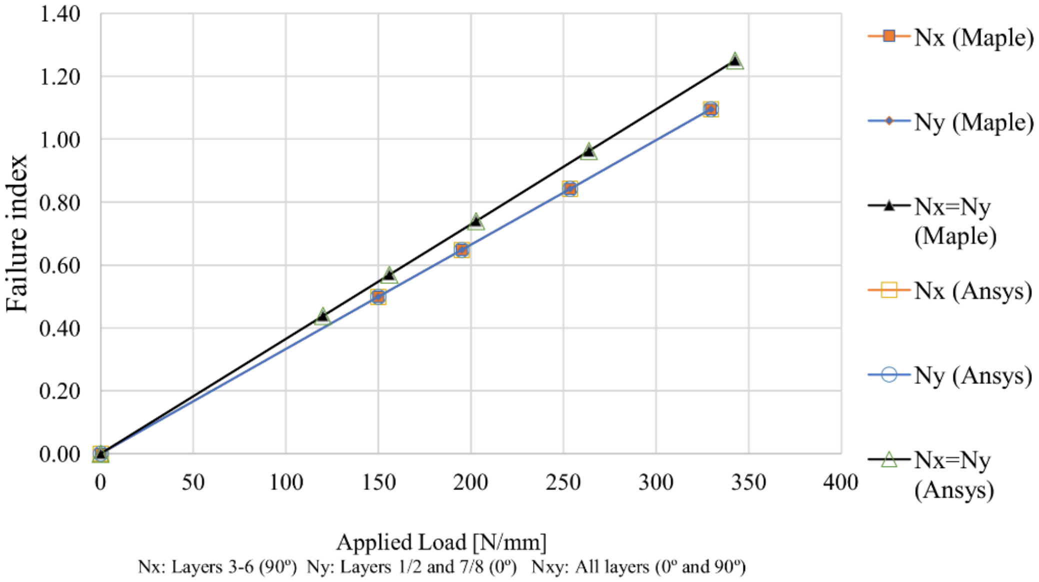

Fig. 3 Comparison of the evolution of Tsai-Wu criterion failure index between analytical (MAPLE®) and numerical (ANSYS® APDL) for laminate E1 ($[0^\circ{}_2/90^\circ{}_2]_S$, AS4/3501-6)

Table 3 presents the applied load values and the respective failure index, considering Tsai-Wu criterion, for the first case, E1. The values of the failure indexes presented in this and in the next tables refer to the layer with the highest failure index value, that is, the layer with the first failure.

In this case, due to the stacking sequence for the uniaxial load situation *N_x*, the laminae with 90^° fibre orientation present higher values of the failure index, denoting a matrix failure. On the other hand, for the load situation *N_y* it is for the laminae with 0^° fibre orientation that present higher values of the failure index, due to, again, the rupture of the matrix. Finally, for the load situation *N_x*=*N_y* it was found that all the laminae, having either 0 and 90 degrees, that constitute the plate, fail simultaneously in the matrix, since equal biaxial loads are considered.

Fig. 3 shows the behaviour of the failure index between the different load situations against the applied force in both the analytical and numerical models. It can be seen that the biaxial loading yields higher Failure index, for an equal load.

For the case of Maximum Stress criterion, similar results are presented in Table 4 and Fig. 4, for the E1 case. It can be concluded that a slighter smaller value of Failure index is found for the N_x and N_y load case but much higher value is found for that parameter in the biaxial case, for the Maximum Stress criterion.

3.2 Laminate E2 ($[30^\circ/90^\circ/-30^\circ/30^\circ]$, Glass/epoxy)

For the laminate E2, one has a non-balanced and non-symmetrical case. The influence of such characteristics in the results is shown in Table 5.

For this case, it was found that, similarly to the previous case, the laminae with the fibres at 90º are affected by the applied load, due to their lower strength, hence it is in this ply where the first

Table 4 Comparison between analytical and numerical (Maximum Stress criterion) approaches (Laminate E1 ($[\mathbf{0^{\circ}{}_2/90^{\circ}{}_2}]_S$, AS4/3501-6)

Analytical					Numerical				
Worst layer	3rd-6th (90°)	1st-2nd (0°)	All (0° and 90°)			3rd-6th (90°)	1st-2nd (0°)	All (0° and 90°)	
	N_x	N_y	$N_x = N_y$			N_x	N_y	$N_x = N_y$	
Load [N/mm]	I_F	I_F	Load [N/mm]	I_F	Load [N/mm]	I_F	I_F	Load [N/mm]	I_F
0	0	0	0	0	0	0	0	0	0
150.0	0.497	0.497	120.0	0	150.0	0.497	0.497	120.0	0.492
195.0	0.645	0.645	156.0	0.492	195.0	0.645	0.645	156.0	0.639
253.5	0.839	0.839	202.8	0.639	253.5	0.839	0.839	202.8	0.831
329.6	1.091	1.091	342.7	1.405	329.6	1.091	1.091	342.7	1.405

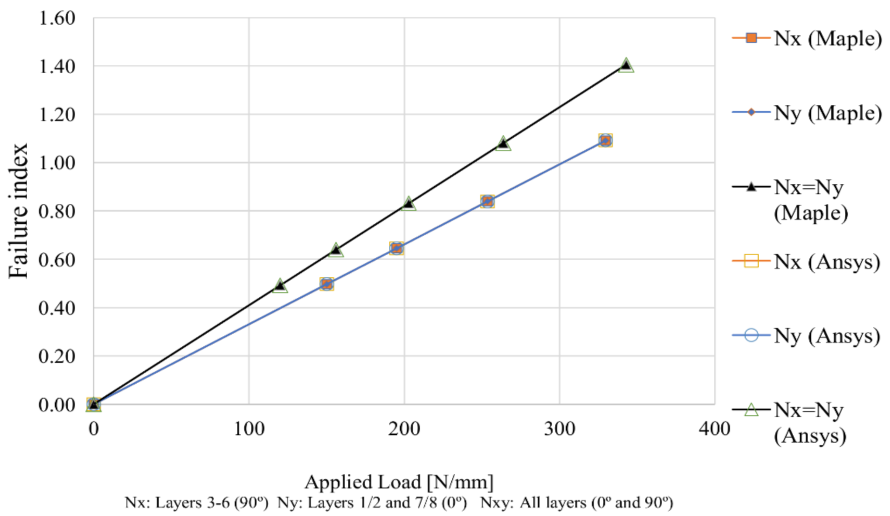

Fig. 4 Comparison of the evolution of Maximum Stress criterion failure index between analytical (MAPLE®) and numerical (ANSYS® APDL) for laminate E1 ($[0^{\circ}{}_2/90^{\circ}{}_2]_S$, AS4/3501-6)

Table 5 Comparison between analytical and numerical (Tsai-Wu criterion) approaches (Laminate E2 ($[\mathbf{30^{\circ}/90^{\circ}/-30^{\circ}/30^{\circ}}]$, Glass/epoxy)

Analytical						Numerical					
Worst layer	2nd (90°)		4th (30°)		1st (30°)		2nd (90°)		4th (30°)		4th (30°)
	N_x		N_y		$N_x = N_y$		N_x		N_y		$N_x = N_y$
Load [N/mm]	I_F	Load [N/mm]	I_F	Load [N/mm]	I_F	Load [N/mm]	I_F	Load [N/mm]	I_F	Load [N/mm]	I_F
0	0	0	0	0	0	0	0	0	0	0	0
30	0.499	31.5	0.500	31	0.500	30	0.480	31.5	0.576	31	0.609
39	0.649	40.9	0.650	40.3	0.650	39	0.624	40.9	0.748	40.3	0.791
50.7	0.826	53.2	0.793	52.4	0.884	50.7	0.791	53.2	0.929	50.7	0.826
65.9	1.096	69.2	1.099	68.1	1.099	65.9	1.054	69.2	1.265	68.1	1.337

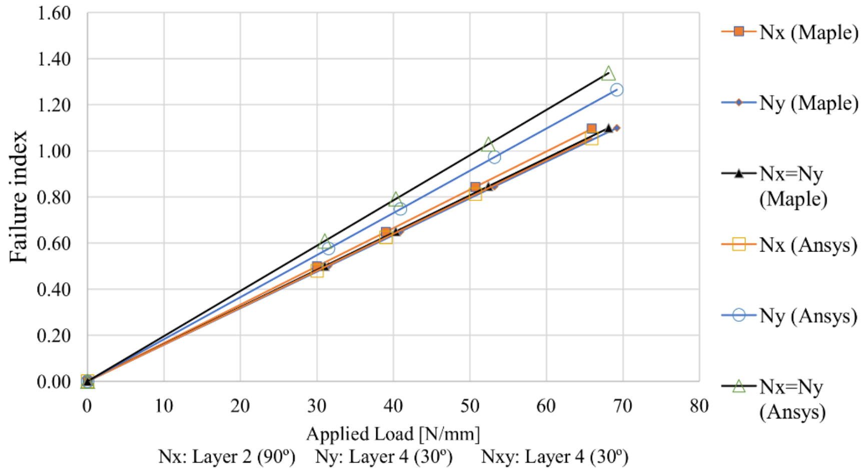

Fig. 5 Comparison of the evolution of Tsai-Wu criterion failure index between analytical (MAPLE®) and numerical ($ANSYS^{®}$ APDL) for laminate E1 ($[30^{\circ}/90^{\circ}/-30^{\circ}/30^{\circ}]$, Glass/epoxy)

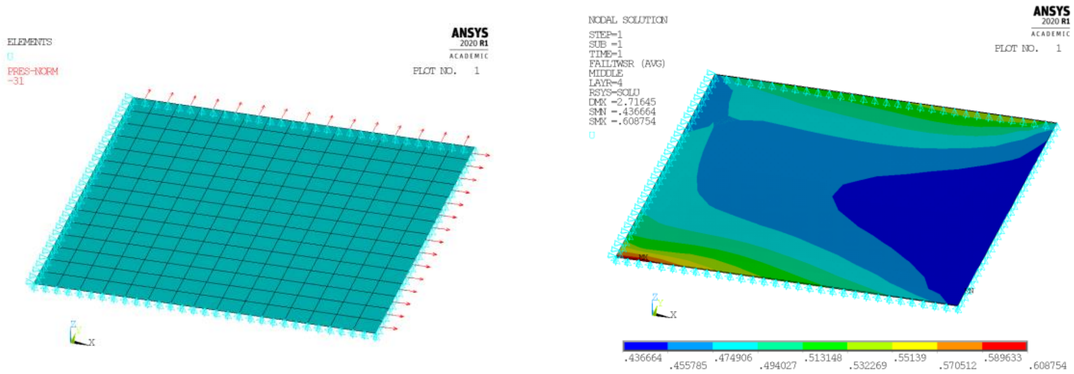

(a) (b)

Fig. 6 (a) Representation of the mesh, supports and loads generated in 2D, for biaxial loading $N_x = N_y$, (b) Illustration of the index failure obtained in the worst ply of the composite for a load of 31 N/mm, for biaxial loading $N_x = N_y$, case E2, layer 4 (30°), using Tsai-Wu failure criterion

Table 6 Comparison between analytical and numerical (Maximum Stress criterion) approaches (Laminate E2 ($[\mathbf{30^{\circ}/90^{\circ}/-30^{\circ}/30^{\circ}}]$, Glass/epoxy)

Analytical						Numerical					
Worst layer 2nd (90°)		4th (30°)		1st (30°)		2nd (90°)		4th (30°)		4th (30°)	
N_x		N_y		$N_x = N_y$		N_x		N_y		$N_x = N_y$	
Load [N/mm]	I_F	Load [N/mm]	I_F	Load [N/mm]	I_F	Load [N/mm]	I_F	Load [N/mm]	I_F	Load [N/mm]	I_F
0	0	0	0	0	0	0	0	0	0	0	0
30	0.489	31.5	0.469	31	0.523	30	0.468	31.5	0.550	31	0.642
39	0.635	40.9	0.609	40.3	0.680	39	0.608	40.9	0.714	40.3	0.835
50.7	0.826	53.2	0.793	52.4	0.884	50.7	0.791	53.2	0.929	52.4	1.085
65.9	1.074	69.2	1.031	68.1	1.149	65.9	1.028	69.2	1.209	68.1	1.411

failure is observed, due to the rupture of the matrix, for the N_x load situation. On the other hand, for the load situation N_y and $N_x = N_y$ the laminae whose fibre orientation is 30º are the most affected by the load, and consequently have the first failure due to the rupture of the matrix, since the load is not applied towards the fibres in these laminae. Fig. 5 shows the behaviour of the failure index of this plate for the different types of loading applied to it.

Contrarily to the previous laminate, the present membrane and membrane-bending stiffness's matrices [A] and [B] are full matrices due to the non-symmetrical and non-balanced character of this laminate, which clearly denotes the bending behaviour of plates when submitted to membrane loadings.

Fig. 6 shows an illustrative image, taken from ANSYS®, with the Tsai-Wu failure index values of the worst laminate layer (30°) for the load situation $N_x = N_y$ and with the load value of 31 N/mm.

For this non symmetric and non-balanced case with out of plane rotations, it was decided to prevent the normal to plane displacements in the border of load application, as seen in Fig. 5.

In Table 6 and Fig. 7 similar analysis results can be seen using the Maximum Stress criterion, in this E2 case. Again, it can be concluded that a slighter smaller value of Failure index is found for the N_x and N_y load case but a higher value is found for that parameter in the biaxial case, for the Maximum Stress criterion. A slightly more dispersed relation between the several load cases is seen in the Maximum Stress criterion (Fig. 7), as the lines diverge more than in the Tsai-Wu criterion (Fig. 5).

3.3 Laminate E3 ($[45^{\circ}/-45^{\circ}]_S$ Glass/epoxy)

The laminate E3 is a balanced and symmetric laminate with only +45 and -45 plies. Its failure index evolution, with the applied load, is presented in Table 7. This table shows that, regardless the

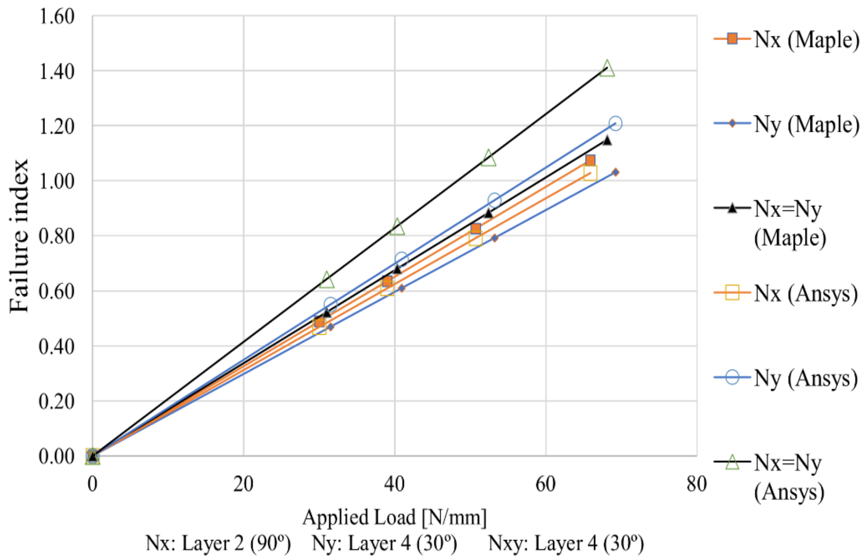

Fig. 7 Comparison of the evolution of Maximum Stress criterion failure index between analytical (MAPLE®) and numerical (ANSYS® APDL) for laminate E2 ($[30^{\circ}/90^{\circ}/-30^{\circ}/30^{\circ}]$, Glass/epoxy)

Table 7 Comparison between analytical and numerical (Tsai-Wu criterion) approaches (Laminate E3 ($[\mathbf{45^{\circ}/-45^{\circ}}]_S$, Glass/epoxy)

Analytical					Numerical				
Worst layer	All	All	All		All	All		All	
	N_x	N_y	$N_x = N_y$			N_x	N_y	$N_x = N_y$	
Load [N/mm]	I_F	I_F	Load [N/mm]	I_F	Load [N/mm]	I_F	I_F	Load [N/mm]	I_F
0	0	0	0	0	0	0	0	0	0
50	0.529	0.529	33	0.449	50	0.529	0.529	33	0.449
65	0.688	0.688	42.9	0.584	65	0.688	0.688	42.9	0.584
84.5	0.894	0.894	55.8	0.759	84.5	0.894	0.894	55.8	0.759
109.9	1.162	1.162	94.25	1.283	109.9	1.162	1.162	94.25	1.283

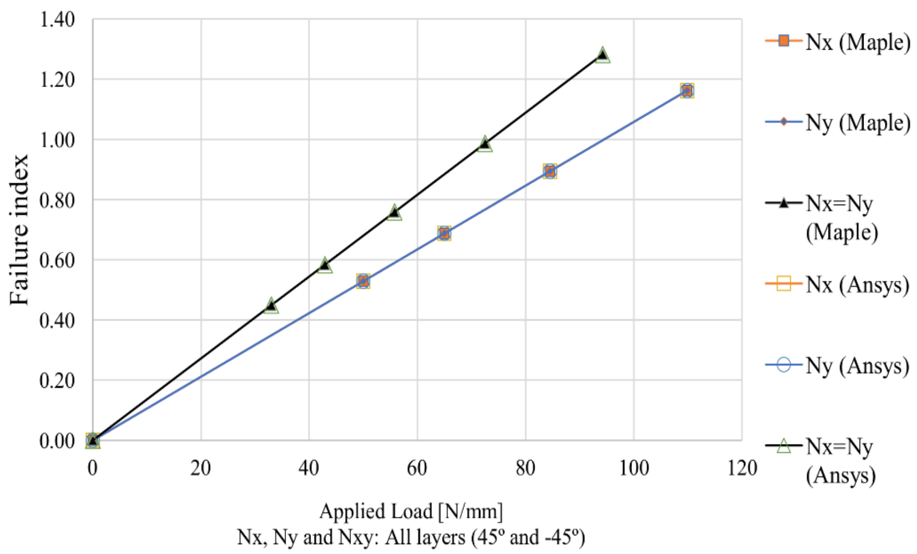

Fig. 8 Comparison of the evolution of Tsai-Wu criterion failure index between analytical (MAPLE®) and numerical ($ANSYS^{®}$ APDL) for laminate E3 ($[45^{\circ}/-45^{\circ}]_S$, Glass/epoxy)

type of loading applied, the laminae fail at the same time for the uniaxial case of N_x and N_y, a behaviour that was expected due to this type of stacking.

With the studies carried out it was concluded that for this type of stacking, both the matrix and the fibre are affected by the load, however posing the fact that the matrix is the weakest, it is the responsible for the failure of the plate. Fig. 8 shows the evolution of the failure index with loading for different types of loading, for this type of stacking. The biaxial loading is more severe in terms of damaging the plate.

The same studies were made using the Maximum Stress criterion and their results are depicted in Table 8 and Fig. 9. Comparing the inclination of curves from Fig. 9 with Fig. 8, the Maximum Stress criterion predicts a lower failure index than the Tsai-Wu criterion, for the same loading, for all the types of loading configurations.

Table 8 Comparison between analytical and numerical (Maximum Stress criterion) approaches (Laminate E3 ($[\mathbf{45^{\circ}/-45^{\circ}}]_S$, Glass/epoxy)

	Analytical				Numerical				
Worst layer	All	All		All		All	All		All
	N_x	N_y		$N_x = N_y$		N_x	N_y		$N_x = N_y$
Load [N/mm]	I_F	I_F	Load [N/mm]	I_F	Load [N/mm]	I_F	I_F	Load [N/mm]	I_F
0	0	0	0	0	0	0	0	0	0
50	0.365	0.365	33	0.482	50	0.366	0.366	33	0.482
65	0.475	0.475	42.9	0.627	65	0.475	0.475	42.9	0.627
84.5	0.618	0.618	55.8	0.815	84.5	0.618	0.618	55.8	0.815
109.9	0.803	0.803	72.5	1.060	109.9	0.803	0.803	72.5	1.060

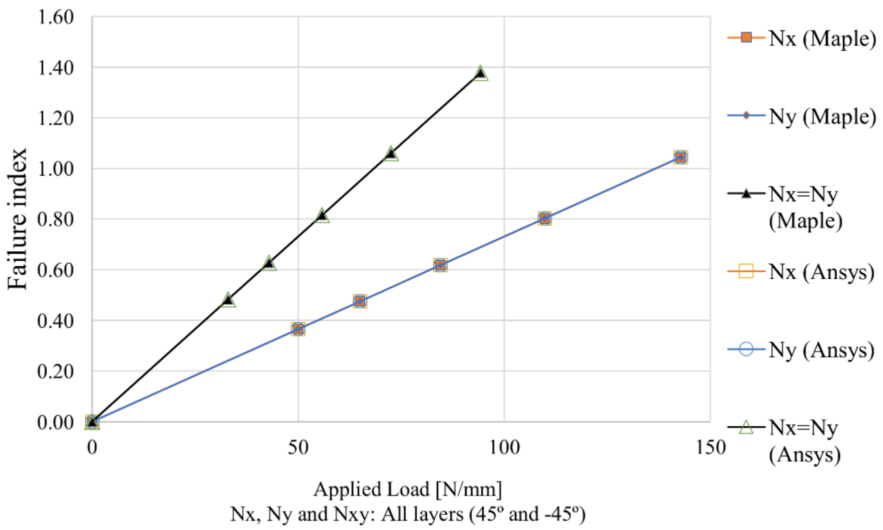

Fig. 9 Comparison of the evolution of (Maximum Stress criterion failure index between analytical (MAPLE®) and numerical ($ANSYS^{®}$ APDL) for laminate E3 ($[45^{\circ}/-45^{\circ}]_S$, Glass/epoxy)

Table 9 Comparison between analytical and numerical (Tsai-Wu criterion) approaches (Laminate E4 ($[\mathbf{0^{\circ}/90^{\circ}/0^{\circ}}]$, Glass/epoxy)

	Analytical					Numerical					
Worst layer	(90°)		(0°)		(0°)		(90°)		(0°)		(0°)
	N_x		N_y		$N_x = N_y$		N_x		N_y		$N_x = N_y$
Load [N/mm]	I_F	Load [N/mm]	I_F	Load [N/mm]	I_F	Load [N/mm]	I_F	Load [N/mm]	I_F	Load [N/mm]	I_F
0	0	0	0	0	0	0	0	0	0	0	0
17	0.502	12	0.493	11	0.460	17	0.502	12	0.493	11	0.460
22.1	0.653	15.6	0.641	14.3	0.598	22.1	0.653	15.6	0.641	14.3	0.598
28.7	0.849	20.3	0.833	18.6	0.777	28.7	0.849	20.3	0.833	18.6	0.777
37.4	1.104	26.4	1.083	24.2	1.011	37.4	1.104	26.4	1.083	24.2	1.011

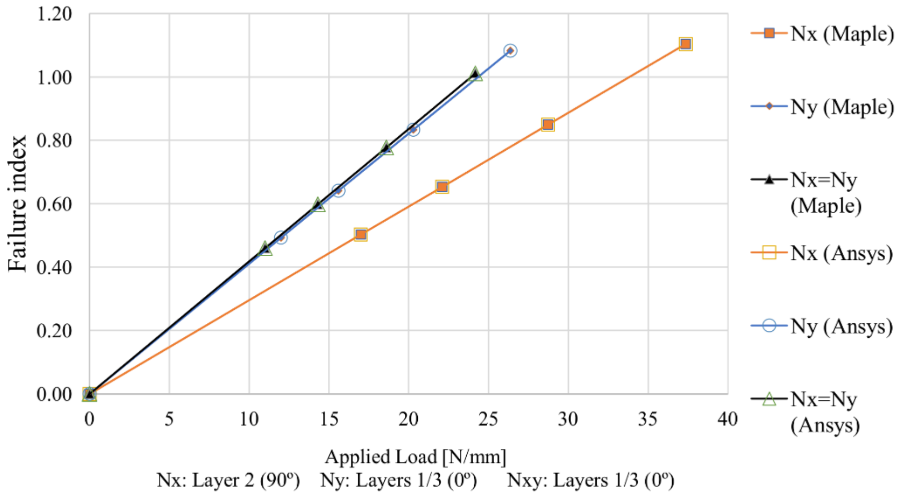

Fig. 10 Comparison of the evolution of Tsai-Wu criterion failure index between analytical (MAPLE®) and numerical (ANSYS® APDL) for laminate E4 ($[0^{\circ}/90^{\circ}/0^{\circ}]$, Glass/epoxy)

Table 10 Comparison between analytical and numerical (Maximum Stress criterion) approaches (Laminate E4 ($[\mathbf{0}^{\circ}/\mathbf{90}^{\circ}/\mathbf{0}^{\circ}]$, Glass/epoxy)

Analytical						**Numerical**					
Worst layer	(90°)		(0°)		(0°)		(90°)		(0°)		(0°)
	N_x		N_y		$N_x = N_y$		N_x		N_y		$N_x = N_y$
Load [N/mm]	I_F	Load [N/mm]	I_F	Load [N/mm]	I_F	Load [N/mm]	I_F	Load [N/mm]	I_F	Load [N/mm]	I_F
0	0	0	0	0	0	0	0	0	0	0	0
17	0.499	12	0.492	11	0.486	17	0.499	12	0.492	11	0.486
22.1	0.649	15.6	0.639	14.3	0.632	22.1	0.649	15.6	0.639	14.3	0.632
28.7	0.843	20.3	0.831	18.6	0.822	28.7	0.843	20.3	0.831	18.6	0.822
37.4	1.096	26.4	1.080	24.2	1.069	37.4	1.096	26.4	1.080	24.2	1.069

3.4 Laminate E3 ($[0^{\circ}/90^{\circ}/0^{\circ}]$, Glass/epoxy)

Resulting from similar studies performed for the laminate E4, one has obtained the values summarized in Table 9 and Fig. 10, for the Tsai-Wu criterion and in Table 10 and Fig. 11 for the Maximum Stress criterion. It can be seen again like the case study E1 and E2, the case of Maximum Stress criterion yields a slighter smaller value of Failure index for the N_x and N_y load case but a higher value is found for that parameter in the biaxial case. Also, that the Ny is closer to the results of the N_{xy} case, for the Tsai-Wu criterion.

3.5 Laminate E3 ($[0^{\circ}/-45^{\circ}/45^{\circ}/90^{\circ}]$, G4-800/5260

Finally, for the last laminate, the simulations performed lead to the results presented in Table 11 and Fig. 12 for the Tsai-Wu criterion and Table 12 and Fig. 13 for the Maximum Stress criterion. It

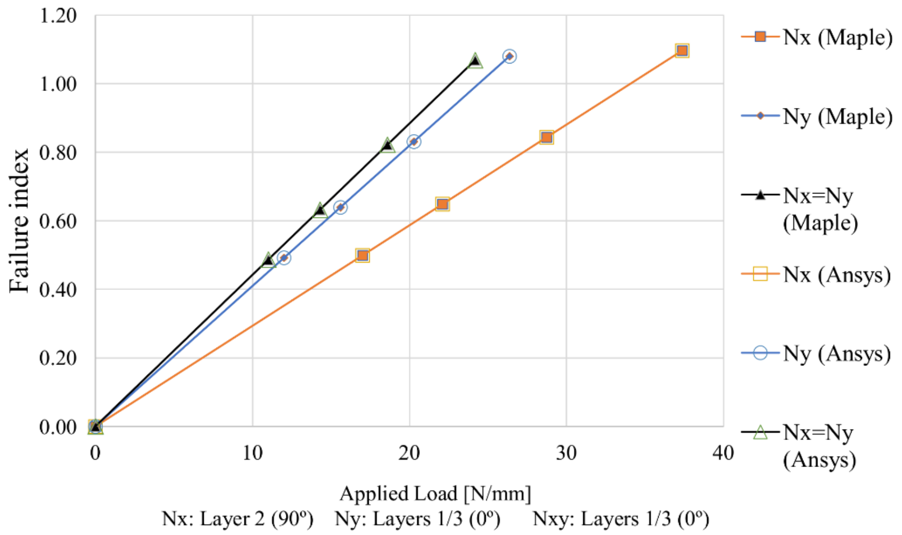

Fig. 11 Comparison of the evolution of Maximum Stress criterion failure index between analytical (MAPLE®) and numerical (ANSYS® APDL) for laminate E4 ($[0^{\circ}/90^{\circ}/0^{\circ}]$, Glass/epoxy)

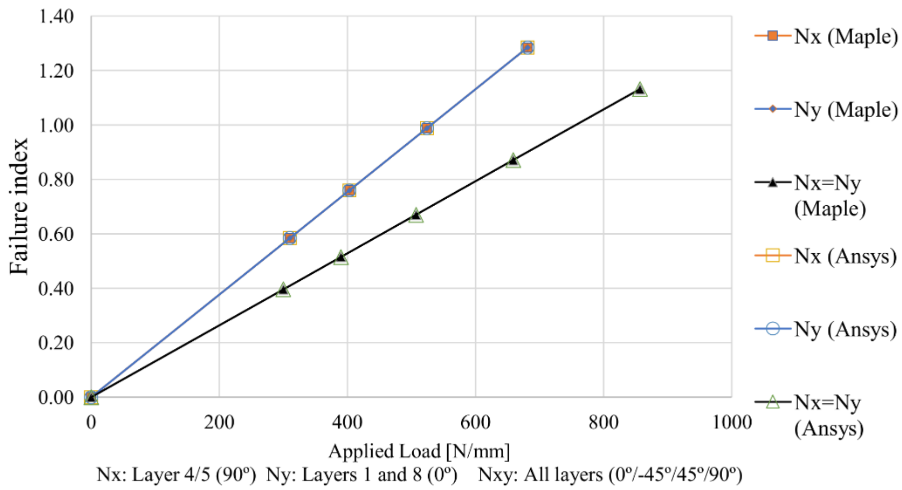

Fig. 12 Comparison of the evolution of Tsai-Wu criterion failure index between analytical (MAPLE®) and numerical ($ANSYS^{®}$ APDL) for laminate E5 ($[0^{\circ}/-45^{\circ}/45^{\circ}/90^{\circ}]_s$,G4-800/5260)

can be seen again like the case study E1, E2 and E4 the case of Maximum Stress criterion yields a slighter smaller value of Failure index for the N_x and N_y load case but a higher value is found for that parameter in the biaxial case. Also, from Fig. 13 it can be seen that the N_x, N_y and the biaxial case curves are quite closer to each other for the Maximum Stress criterion.

With these results it was concluded that the results obtained present the same pattern behaviour identified for the previous symmetric laminates. As in other studies, for this case of laminate E5 it was found that the laminae that have the fibres with a 90º orientation angle suffer more with the uniaxial loading N_x, while the laminae that have the fibres with an orientation angle of 0º suffer

Table 11 Comparison between analytical and numerical (Tsai-Wu criterion) approaches (Laminate E5 ($[\mathbf{0}^{\circ}/-\mathbf{45}^{\circ}/\mathbf{45}^{\circ}/\mathbf{90}^{\circ}]_s$, G4-800/5260)

Analytical					Numerical				
Worst layer	4th and 5th (90°)	1st and 5th (0°)	All		4th and 5th (90°)	1st and 5th (0°)	All		
	N_x	N_y	$N_x = N_y$			N_x	N_y		$N_x = N_y$
Load [N/mm]	I_F	I_F	Load [N/mm]	I_F	Load [N/mm]	I_F	I_F	Load [N/mm]	I_F
0	0	0	0	0	0	0	0	0	0
310.0	0.585	0.585	300	0.396	310.0	0.585	0.585	300.0	0.396
403.0	0.760	0.760	390	0.515	403.0	0.760	0.760	390.0	0.515
523.9	0.988	0.988	659	0.871	523.9	0.988	0.988	659.1	0.871
681.1	1.285	1.285	857	1.132	681.1	1.285	1.285	856.8	1.132

Table 12 Comparison between analytical and numerical (Maximum Stress criterion) approaches (Laminate E5 ($[\mathbf{0}^{\circ}/-\mathbf{45}^{\circ}/\mathbf{45}^{\circ}/\mathbf{90}^{\circ}]_s$, G4-800/5260)

Analytical					Numerical				
Worst layer	4th and 5th (90°)	1st and 5th (0°)	All		4th and 5th (90°)	1st and 5th (0°)	All		
	N_x	N_y	$N_x = N_y$			N_x	N_y		$N_x = N_y$
Load [N/mm]	I_F	I_F	Load [N/mm]	I_F	Load [N/mm]	I_F	I_F	Load [N/mm]	I_F
0	0	0	0	0	0	0	0	0	0
310.0	0.501	0.501	300	0.501	310.0	0.501	0.501	300	0.501
403.0	0.652	0.652	390	0.651	403.0	0.652	0.652	390	0.651
523.9	0.847	0.847	507	0.847	523.9	0.847	0.847	507	0.847
681.1	1.101	1.101	659.1	1.101	681.1	1.101	1.101	659.1	1.101

more for the uniaxial loading N_y. Fig. 8 depicts the behaviour of the failure index with loading for case E5.

3.5 Deviations' characterization

From the results obtained for the set of simulations performed it is additionally pertinent to consider the deviations between some results obtained via the numerical and analytical approaches. To this purpose the deviation is determined as

$$dev = \left| \frac{IF_{Numerical} - IF_{Analytical}}{IF_{Analytical}} \right| * 100\% \tag{12}$$

Table 13 shows the maximum relative deviations found for some cases. The loading type and its value are also presented.

Analysing the results presented in Table 13, it can be concluded that there are no differences between most of the results obtained with the developed models. However, for the laminate E2 the

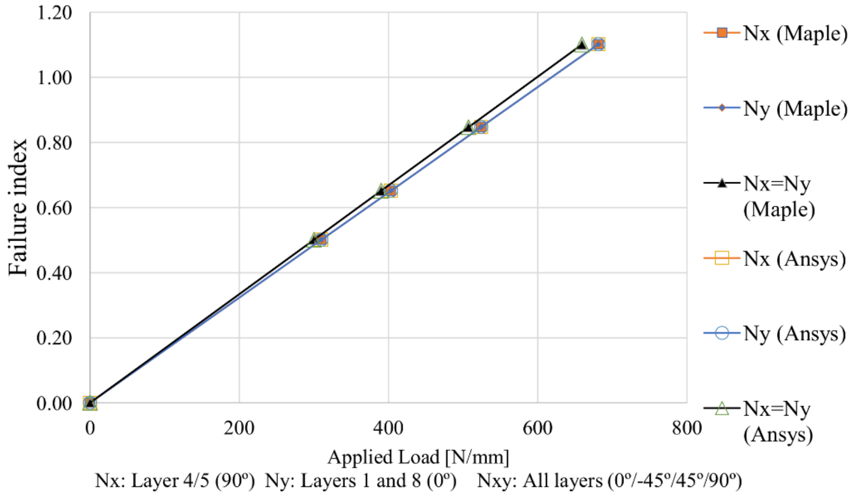

Fig. 13 Comparison of the evolution of Maximum Stress criterion failure index between analytical (MAPLE®) and numerical (ANSYS® APDL) for laminate E5 ($[0^{\circ}/-45^{\circ}/45^{\circ}/90^{\circ}]_s$, G4-800/5260)

Table 13 Comparison between the results obtained in numerical (N) and analytical (A) models for some loading cases

	Laminate E1	Laminate E2	Laminate E3	Laminate E4	Laminate E5
Load situation	N_x *or* N_y	$N_x + N_y$	N_x or N_y	$N_x + N_y$	N_x or N_y
Load (A) [N/mm]	329.6	68.1	142.8	24.2	681.1
FI	1.091	1.099	1.044	1.011	1.101
Criterion	Tsai-Wu	Tsai-Wu	Max. Stress	Tsai-Wu	Max. Stress
Load (N) [N/mm]	329.6	52.4	142.8	24.2	681.1
FI	1.091	1.029	1.044	1.011	1.101
Criterion	Tsai-Wu	Tsai-Wu	Max. Stress	Tsai-Wu	Max. Stress
Deviation (%)	0	-23.05	0	0	0

value of the deviation is significant. This may be attributed to the plate's non-balanced and non-symmetrical stacking sequence, which causes distortion on the plane and out of plane curvatures (see Fig. 6(b)). This pattern behaviour was already reported by (Camilleri *et al.* 2014).

Further studies using other failure criteria like Hashin, Puck etc could be considered to see if a better relation is obtained between analytical and numerical methods. Additionally, an experimental validation campaign could also be considered.

5. Conclusions

This work considered the failure of laminated plates submitted to uniaxial and biaxial tensile loads, considering two failure criteria: Tsai-Wu and Maximum Stress. Parametric studies were developed to characterize the influence of material and geometrical parameters on the failure index and/or strength ratio.

It was observed that the load of the first failure depends on the orientation of the fibres, on the thickness of each lamina, and on the number of layers, besides the mechanical properties of the materials involved.

For the uniaxial loading N_x and for the cases analysed it was possible to conclude that laminates E1 and E5 cases present a higher strength when compared to the laminates E2, E3, and E4. This is visible by their lower first ply failure loads and is mainly due to the stronger material employed (carbon fibre). Laminate E4 showed to present the lowest first failure load in all studies, due to the lower number of plies and lower ply thickness and less strong reinforcing material (glass fibre). It was also found that plies whose fibres had a 90° orientation, presented a first failure due to the matrix failure. For the uniaxial loading (N_y) an inverse behaviour was observed, which was an expected result. The better performing laminate showed to be the E5, with a first failure load of 681.1N/mm, against the worst performing, the E4 laminate, with a first ply failure load of 26.4 N/mm.

For the biaxial loading case, with N_x=N_y it was found that the laminate E5 had again a greater strength, presenting a first ply failure load of 659.1 N/mm, while the E4 one was in the opposite side with a failure load of 24.2 N/mm. For these loading cases, it was observed that regardless of the load value and the orientation of the fibres, all the laminae presented failure and similar failure indexes, that is, theoretically the laminae would fail at the same time.

It was also observed that the non-balanced non-symmetrical laminate sequence E2 presented a completely different behaviour from the symmetrical and balanced laminate sequences, with higher differences between numerical and analytical models. However, a deepened study for this case should be made considering other composite failure criteria and experimental testing.

Acknowledgments

The first author would like to acknowledge SAS (Serviços de Acção Social) of IPL (Instituto Politécnico de Lisboa) and the Instituto Superior de Engenharia de Lisboa for providing the necessary tools develop this work.

The authors wish to acknowledge the support given by FCT/MEC through Project IDMEC, LAETA UIDB/50022/2020.

References

ANSYS Student Release 2020 Documentation (2020), Swanson Analysis Systems Inc.

Aydogdu, M. (2008), "Conditions for functionally graded plates to remain flat under in-plane loads by classical plate theory", *Compos. Struct.*, **82**(1), 155-157. https://doi.org/10.1016/j.compstruct.2006.10.004.

Barbero, E.J. (2007), *Finite Element Analysis of Composite Materials* (1st ed.), CRC Press.

Cabrero, J.M. and Gebremedhin, K.G. (2010), "Evaluation of failure criteria in wood members", *Proceedings of the 11th World Conference on Timber Engineering 2010*, WCTE 2010, **2**, 1274-1280.

Camilleri, D., Ellul, B. and Muscat, M. (2014), "Design-by-analysis methods for asymmetric or unbalanced cylindrical composite pressure vessels", *Proceedings of the ASME 2014 Pressure Vessels and Piping Conference*, **3**, 1-8.

Dent, A.H. and Sherr, L. (2014), *Material Innovation: Product Design*, Thames and Hudson.

Flatscher, T., Schuecker, C. and Pettermann, H.E. (2013), "A constitutive ply model for stiffness degradation and plastic strain accumulation: Its application to the third world wide failure exercise (Part A)", *J. Compos. Mater.*, **47**(20-21), 2575-2593. https://doi.org/10.1177/0021998313484075.

Hinton, M.J., Kaddour, A.S. and Soden, P.D. (2004), *Failure Criteria in Fibre Reinforced Polymer*

Composites: The World-Wide Failure Exercise, Elsevier.
Kaddour, A.S. and Hinton, M.J. (2013), "Maturity of 3D failure criteria for fibre-reinforced composites: Comparison between theories and experiments: Part B of WWFE-II", *J. Compos. Mater.*, **47**(6-7), 925-966. https://doi.org/10.1177/0021998313478710.
Kaddour, A.S., Hinton, M.J., Smith, P.A. and Li, S. (2013), "The background to the third world-wide failure exercise", *J. Compos. Mater.*, **47**(20-21), 2417-2426. https://doi.org/10.1177/0021998313499475.
Kaddour, A.S., Hinton, M.J., Li, S. and Smith, P.A. (2014), "The world-wide failure exercises: How can composites design and manufacture communities build their strength", *Proceedings of the 16th European Conference on Composite Materials*, ECCM 2014, Seville, Spain.
Kim, C.W., Song, S.R., Hwang, W., Park, H.C. and Han, K.S. (1994), "On the failure indices of quadratic failure criteria for optimal stacking sequence design of laminated plate", *Appl. Compos. Mater.*, **1**(1), 81-85. https://doi.org/10.1007/BF00567214.
Koc, M., Sonmez, F.O., Ersoy, N. and Cinar, K. (2016), "Failure behaviour of composite laminates under four-point bending", *J. Compos. Mater.*, **50**(26), 3679-3697. https://doi.org/10.1177/0021998315624251.
Koh, R. and Madsen, B. (2018), "Strength failure criteria analysis for a flax fibre reinforced composite", *Mech. Mater.*, **124**, 26-32. https://doi.org/10.1016/j.mechmat.2018.05.005.
Li, S. and Sitnikova, E. (2018), "A critical review on the rationality of popular failure criteria for composites", *Compos. Comm.*, **8**, 7-13. https://doi.org/10.1016/j.coco.2018.02.002.
Liu, K.S. and Tsai, S.W. (1998), "A progressive quadratic failure criterion for a laminate", *Compos. Sci. Technol.*, **58**(7), 1023-1032. https://doi.org/10.1016/S0266-3538(96)00141-8.
Nyambeni, N. and Mabuza, B.R. (2018), "Considerations of failure analysis in a multi-layered composite structure under thermomechanical loading", *Multidisciplinary Digital Publishing Institute Proceedings*, **2**(8), 447.
París, F. (2001), "A study of failure criteria of fibrous composite materials", NASA/CR- 2001-210661.
Reddy, J.N. (1997), *Mechanics of Laminated Composite Plates and Shells: Theory and Analysis*, CRC Press.
Saravanan, T.J., Gopalakrishnan, N. and Hari, B.K (2019), "Damage identification in structural elements through curvature mode shapes and nonlinear energy operator", *Compos. Mater. Eng.*, **1**(1), 33-48. https://doi.org/10.12989/cme.2019.1.1.033.
Soden, P.D., Hinton, M.J. and Kaddour, A.S. (1998), "Lamina properties, lay-up configurations and loading conditions for a range of fibre-reinforced composite laminates", *Compos. Sci. Tech.*, **58**(7), 1011-1022. https://doi.org/10.1016/B978-008044475-8/50003-2.
Tsai, S.W. and Wu, E.M. (1971), "A general theory of strength for anisotropic materials", *J. Compos. Mater.*, **5**(1), 58-80. https://doi.org/10.1177/002199837100500106.

GY